2018 Advanced Maui Optical and Space Surveillance Technologies Conference
Maui, HI, USA

OPTIMIZATION OF GEOSYNCHRONOUS SPACE SITUATIONAL AWARENESS ARCHITECTURES USING PARALLEL COMPUTATION

Michael S. Felten[1], **John M. Colombi**[2], **Richard G. Cobb**[3], **and David W. Meyer**[4]

[1] *Air Force Institute of Technology (AFIT), 2950 Hobson Way WPAFB, OH 45433, 507-319-0403, michael.s.felten.mil@mail.mil*

[2] *AFIT, 2950 Hobson Way WPAFB OH 45433, 937-255-3636 ext. 3347, john.colombi@afit.edu*

[3] *AFIT, 2950 Hobson Way WPAFB OH 45433, 937-255-3636 ext. 4559, richard.cobb@afit.edu*

[4] *AFIT, 2950 Hobson Way WPAFB OH 45433, 937-255-3636 ext. 4512, david.meyer@afit.edu*

Keywords: *GEO, SSA, design, optimization, architecture*

PRESENTING AUTHOR: MICHAEL FELTEN

Major Michael Felten graduated in March of 2018 from the Air Force Institute of Technology (AFIT) with a Master's of Science in Systems Engineering and a Master's Space Systems certificate. His research focused on modeling ground and space-based telescopes, simulation of executable architectures, multi-objective optimization, and trade space evaluation. Prior to AFIT, he worked in several acquisition and operational satellite program offices. He was commissioned in the Air Force as a Second Lieutenant in 2006 after graduating from Iowa State University with a Bachelor's Degree in Aerospace Engineering and a minor in Military Studies.

ABSTRACT

Maintaining Space Situational Awareness (SSA) of the operational activities in the space domain remains one of the Department of Defense's (DoD's) top priorities. In the ever increasing congested and contested space environment, assuring operators and maintainers have the right mix of sensors to meet SSA requirements is paramount. Current research at the Air Force Institute of Technology (AFIT) has shown that modeling and simulation of Geosynchronous orbit (GEO) SSA architectures can provide utility in identifying optimal combinations of ground and space-based sensors. These SSA architectures were scored in value based on combined sensor performance and total system cost. This paper extends previous GEO SSA research by expanding design boundaries and refining the methodology.

Specifically, for this paper, a GEO SSA scenario was explored. The updated model increased the inherent value of a selected architecture by nearly 50%. This was accomplished through a more refined examination of an increased trade space

containing 10^{22} possible sensor combinations. High-performance computing capabilities allow parallel evaluation of thousands of architecture combinations at once to significantly reduce the wall time when solving large-scale optimization problems. Experimental trials that would have taken over 100 years on a desktop computer were completed in weeks using a high-performance computer containing over 125,000 cores. Discrete telescope aperture sizes, number of telescopes per location, possible ground locations, and satellite orbital regimes were used as inputs for the optimizer. A multi-objective genetic algorithm intelligently searched the trade space to identify optimal executable architectures.

The results of the optimization clearly favored 1.0-meter aperture ground telescopes combined with 0.15-meter aperture sensors in a 12 satellite Geosynchronous Polar Orbit (GPO) constellation. The 1.0-meter aperture ground telescopes have the best cost-performance combination for detecting Resident Space Objects (RSOs) in GEO. The GPO regime offers increased access to RSOs in GEO, without the 40° solar exclusion angle of lower inclination orbits. When performance is held constant, a GPO satellite constellation offers a 22.4% reduction in total system cost when compared to Sun Synchronous Orbit (SSO), Equatorial Low Earth Orbit (LEO), and near-GEO constellations.

The results of the research can be used to educate national policy makers on the costs and benefits of various proposed upgrades to the current and future SSA architectures. The methodology refined through this research has greater utility than simply GEO SSA architecture evaluation; it can be used as a source selection tool to evaluate opposing contractor bids, a simulation tool for efficient evaluation of very large trade spaces, or an analysis workbench for comparison of emerging technologies. Scripting and parallel high-performance computing opens the possibility of solving an entirely new class of problems of interest to the DoD.

PRESENTATION

The presentation of this material is focused on the results obtained through this research. A brief history of the problem along with the research objectives is outlined during the beginning of the presentation to set the stage for the results that follow. The process used to develop and refine the methodology is outlined in sufficient detail to provide confidence in the results. The results from prior and current data sets are analyzed and compared with each other. The final results identify the optimal architecture parameters with the associated performance and cost estimates.

SUGGESTED SESSIONS

- Space Situational Awareness
- High Performance Computing Applications for Space Surveillance
- Modeling

I. Introduction

Recent reusable rocket technology and the miniaturization of satellite subsystems have enabled cheaper access to the space domain (Früh & Jah, 2014). This trend is increasing the number of operational satellites in space. In 2017, India launched 104 satellites into Low Earth Orbit (LEO) from a single rocket (Barry, 2017). More efficient access to space drives the need for increased Space Situational Awareness (SSA) to minimize the likelihood of an unintentional collision. Geosynchronous orbit (GEO) is of particular interest because of the utility of a 23 hour and 56 minute orbital period (Marlow et al., 2017). This research focuses on modeling and simulation of ground and space-based optical sensors in order to identify optimal sets of architectures to best enable persistent coverage of all the Resident Space Objects (RSOs) in GEO.

The space domain has grown from a force multiplier to a warfighting domain itself (Smith, 2017). The proposed establishment of a dedicated sixth branch of the military specifically focused on the space domain exemplifies the importance of this domain to the Nation. Like land, sea, and air, space will be a domain with future struggles for dominance. The ability to have insight into tactics, techniques, and procedures of our adversaries is paramount. Persistent SSA is the foundational requirement needed to ensure accountability of any malicious activity in space (Dacres, 2016). Maintaining near continuous coverage of the GEO belt serves as a deterrent and protects high-value GEO assets. High-fidelity SSA protects future exploitation of the GEO belt for satellite operation. A satellite breakup in GEO could propagate space debris throughout the orbit causing a cascading effect that effectively eliminates the possibility of any satellite operation in that orbital regime (Tanaka, 2017). It should be the priority of every space fairing nation to operate space vehicles in a manner that reduces the possibility of unintended collisions in space.

All Resident Space Objects (RSOs) larger than 10 cm are currently tracked via the United States Space Surveillance Network (SSN). Figure 1 illustrates the approximated 29,000 objects in orbit greater than 10 cm (Wiedemann, 2018).

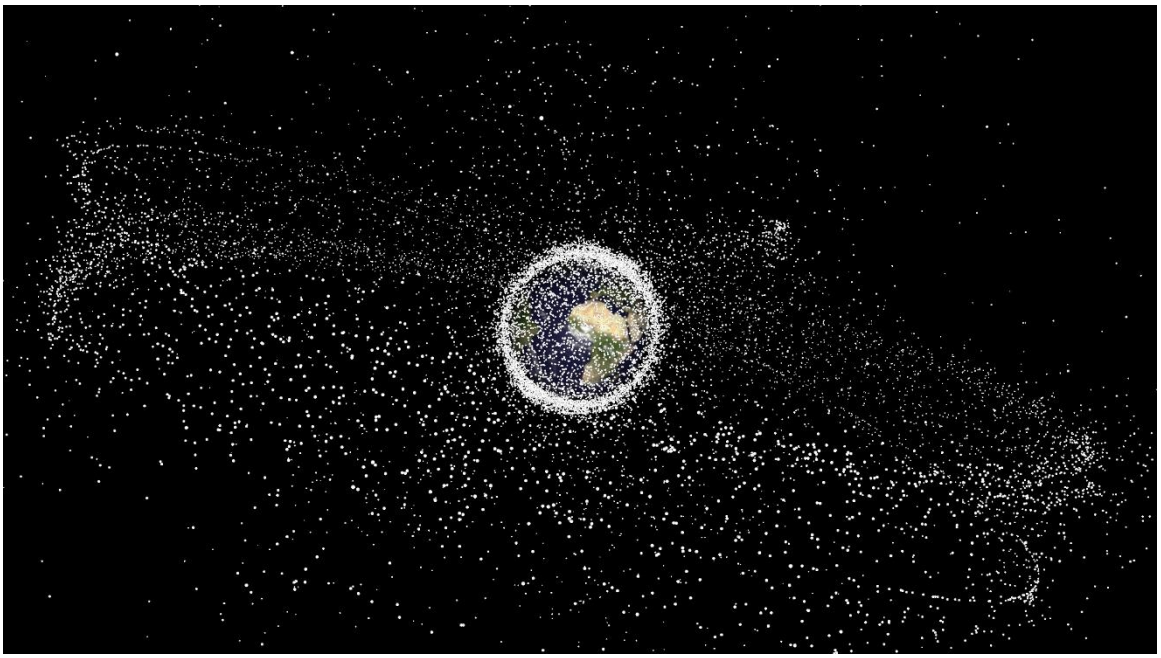

Figure 1. Space objects larger than 10 cm. Used with permission (Wiedemann, 2018)

A 10 cm threshold for RSO tracking was selected because the current system cannot consistently detect and track objects smaller than 10 cm (M. Baird, 2013). However, objects as small as 1 mm carry enough energy—traveling at 4 kilometers per second—to cripple an operational satellite (Tanaka, 2017). Since these objects are not actively tracked, satellite operators do not have orbital predictions that could provide warning of a close approach. Because of this, objects smaller than 10 cm pose the greatest passive threat to today's operational satellites. Figure 2 visually illustrates the predicted number of objects 1 mm or larger currently in orbit.

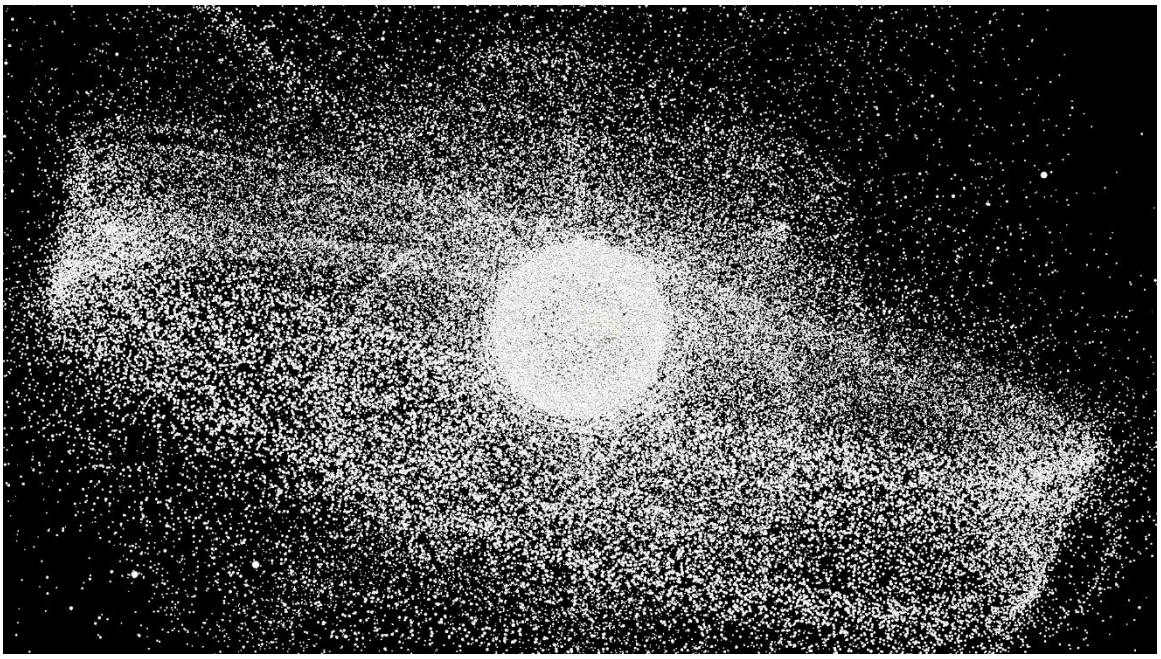

Figure 2. Space objects larger than 1 mm. Used with permission (Wiedemann, 2018)

The newest Air Force space-based SSA sensor, Operationally Responsive Space-5 (ORS-5), launched in August of 2017 (Clark, 2017). Also known as SensorSat, this satellite operates in an equatorial LEO designed to maximize the detection capabilities of GEO RSOs. When this sensor becomes operational, it will improve the SSN's ability to maintain custody of the current GEO space catalog (Brissett, 2017). In 2018, the re-introduction of the Air Force's Space Fence will dramatically improve detection capabilities of small RSOs in GEO. Together, these will complement the existing SSA provided by the Ground-Based Electro-Optical Deep Space Surveillance (GEODDS) network, the Space Surveillance Telescope (SST), the Space-Based Space Surveillance (SBSS) satellite, and the Geosynchronous Space Situational Awareness Program (GSSAP).

Even with the inclusion of SensorSat and Space Fence, the ability to adequately detect and track all RSOs of interest may be insufficient. Gaps in coverage and a lack of capable assets to maintain custody of RSOs have been reported as the two biggest factors of concern regarding the current SSN (Abbot & Wallace, 2007). Additional sensors may be needed to enable persistent coverage of all the RSOs in GEO. However, the optimal number, telescope aperture size, ground location, orbital plane, and type of sensor(s) required is unknown (Tanaka, 2017).

The purpose of this research was to propose an optimal architecture for effective and efficient GEO SSA and determine how that architecture performs throughout the year. An ideal solution minimizes the latency between subsequent RSO collects and

minimizes the detectable object size, while minimizing cost. Primarily this research used modeling and simulation through vast trade space analysis to determine what combination of ground and space-based sensors provide the most cost-effective architecture for a high-fidelity GEO SSA system. Secondly, the research determined how the optimal architecture changed throughout the year because of Earth-Sun angle variations.

This research builds upon previous results using a Multi-Objective Genetic Algorithm (MOGA) that identified near-optimal GEO SSA architectures for two specific days of the year: the summer solstice and spring equinox (Stern et al., 2017). Refinement and enhancement of this methodology was shown to increase the efficiency of the dynamic simulation used for generation and evaluation of executable architectures (Garcia & Tolk, 2015). These enhancements facilitated an expansion of the previous design space by 1,000 times. The new design space is shown graphically in Figure 3.

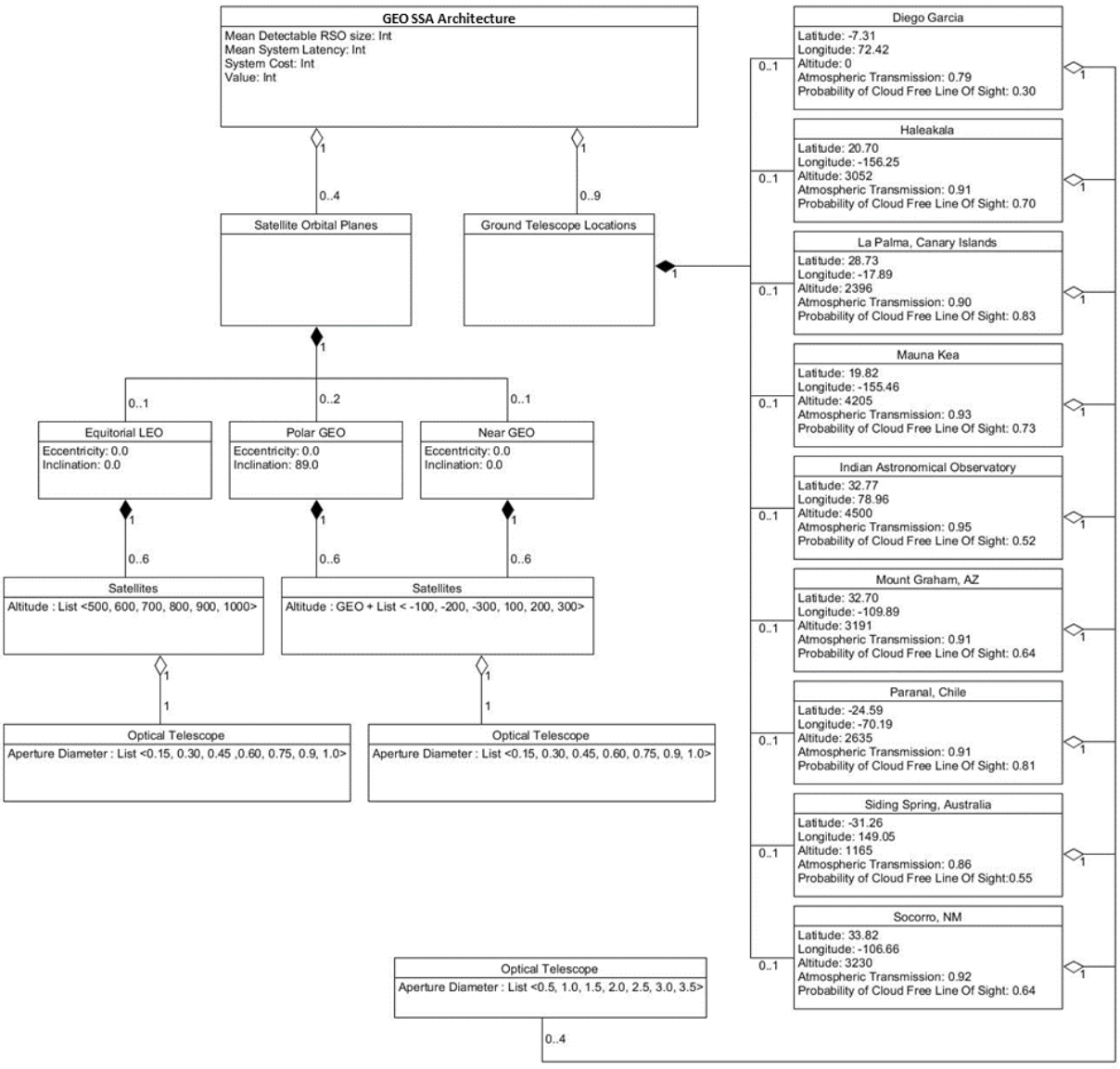

Figure 3. Revised SSA Architectural Elements and Design Space

Development and refinement of the integrated toolset was required to efficiently search a design space containing 10^{22} possible combinations of architectural elements. The complete toolset includes Python and Linux scripting, AGI's Systems Tool Kit Engine (STKE), an open source MOGA implementation, and a High-Performance Computer (HPC). This toolset can be used as an analysis workbench for diverse types of evaluation for very large trade spaces. The results of the research can be used to inform policy makers and budget authorities about the most cost-effective means to achieving a persistent GEO SSA capability. Cost constraints and performance targets can be easily modified to generate new tailored optimal architectures. Modifications to the input parameters enable analysis of emerging technologies and could be used as a source selection tool to evaluate proposals to focus program funding. The possible applications of this research to future space and non-space related modeling and simulation applications is boundless.

II. Background

Space has become an increasingly important domain for the United States, both economically and militarily. Conflict in this domain is inevitable (John, 2002) and ensuring the survival of the currently 1400 operational satellites (Tanaka, 2017) through any future conflict is critical. This research focuses on several concepts, including: computational analysis, space modeling, architecture design, cost analysis, performance simulation, parallel evaluation of executable architectures, and multi-objective optimization.

The threat of Intercontinental Ballistic Missiles (ICBM) in the Cold War required the United States to build massive radar stations in the Northern Hemisphere. After the collapse of the Soviet Union, these radar stations were under-utilized. At the same time, space was getting more crowded so these radar sites began working on the SSA mission (M. Baird, 2013). This method of RSO detection vastly improved the tracking capability of RSOs in LEO (Ackermann, Kiziah, Zimmer, McGraw, & Cox, 2015). However, the effectiveness of radar is drastically reduced as the distance to the object is increased. This limitation makes these radar sites only effective for the LEO SSA mission.

Complementing the detection of RSOs through missile warning radar sites, optical telescopes are used to detect reflected light—usually from the Sun—off an RSO. Because optical telescopes are passive sensors, they do not suffer from the distance limitations as drastically as radar sensors. It follows that optical sensors are the ideal instrument for GEO SSA. Detection of any RSO requires a high signal-to-noise ratio with respect to the background. A typical value of 2.5 is large enough to ensure detection through an optical telescope (Früh & Jah, 2014). There are two ways an optical telescope can be used to detect RSOs. If the orbital parameters of the object are known, the telescope can track that object across the sky and measure the streaks of light generated by the stars in the background to back out that RSO's orbital elements. Alternatively, the telescope can fix its position on the background stars. In this instance, the streak of light through the frame can be used to calculate the RSO's orbital parameters (Dacres, 2016).

Optical telescopes operating as a payload on an orbiting satellite function in a very similar manner to ground-based telescopes but with several inherent advantages. Weather and other atmospheric interference is not an issue for an orbiting platform. The system can operate 24/7 as opposed to the nighttime only operation of current ground-based telescopes. However, a solar exclusion angle exists for all space

sensors that limits the sensor's Field of Regard (FOR) to within a defined threshold of the solar disk (Scott et al., 2013).

There are particular orbital regimes that enable increased detection opportunities for GEO RSOs. This research explores a polar orbit at an altitude similar to GEO in order to minimize the effect of the solar exclusion angle. The geometry of a Geosynchronous Polar Orbit (GPO) satellite provides increased access for targeting RSOs in the GEO belt. Another orbital regime that offers increased detection capability is LEO with zero inclination. This orbit allows increased exposure time when detecting objects in GEO since the satellite platform is in the same plane as most of the target RSOs. This provides a 10x improvement in detection opportunity (Ackermann et al., 2015). A near GEO satellite has the advantage of being very close to GEO RSOs and therefore has an enhanced detection capability. All three of these orbits were considered for this research since they potentially have enhanced utility for the GEO SSA mission.

In today's budget-constrained environment, cost is a major consideration for every program. Two questions drive future funding and technology development: What type of platforms provide the greatest operational capability, and what combination of sensors provide the greatest utility? This research was a continuation of previous optimal design using lifecycle cost (LCC) as one of multiple objectives to optimize. LCC includes development cost, procurement cost, launch cost, operation and sustainment cost, and disposal cost of these solutions (Stern et al., 2017).

The cost models for space-based optical telescopes scale linearly with the weight of the satellite, and the weight of the satellite scales linearly with the aperture diameter (Stahl, Henrichs, & Luedtke, 2011). Thus, the aperture size of any space-based observation satellite can be used as a design parameter in this cost model. A similar form of cost estimation can be used to obtain ground telescope cost estimates. Optical observatories built for astronomical observation have an estimated total cost that scales with aperture diameter raised to the 2.45 power (Van Belle, Meinel, & Meinel, 2004). These cost estimates can then be used to identify an approximate cost for each system based upon how many ground and space-based assets are included. Other estimates used to refine the final cost model include: Unmanned Space Vehicle Cost Model (USCM), the Small Satellite Cost Model (SSCM), the NASA Instrument Cost Model (NICM), and the NASA Operations Cost Model (NOCM) (Stern et al., 2017).

There is nearly an infinite combination of sensors that could be used to accomplish the SSA mission. Because of the large number of variables in this analysis coupled with lengthy simulation time for each candidate solution, the best optimization technique is one that can be run most efficiently parallelized. This allows solutions to be found in a reasonable timeframe. The DoD Supercomputing Resource Center (DSRC) and their HPC capabilities allow parallel evaluation of thousands of architecture combinations at once and significantly reduces the wall time when solving large-scale optimization problems (Thompson et al., 2015). This was identified as a limiting factor in previous research attempting to identify optimal space architectures (Stern et al., 2017). In that SSA architecture study, the trade space contained 10^{19} combinations of ground-based and space-based assets. Evaluation of every architecture is not possible with such a high number of possible sensor combinations. A heuristic search method to efficiently evaluate the trade space is required. Even with utilization of a heuristic search algorithm, the HPC is a critical component of this methodology. Without the computational resources the HPC provides, evaluation of complex SSA architectures using this approach would take decades.

III. Methodology

The method used for this research involves accurately modeling and simulating the orbital dynamics of 813 Resident Space Objects (RSOs) in GEO, ground telescope performance at various locations, and space-based sensors in varying orbits (Stern et al., 2017). This simulates a ground or on-orbit sensor attempting to detect and track objects in the GEO belt. Advanced algorithms are then used to sort, schedule, and then optimize the sensor selection based on a defined criteria. This methodology can be divided into several steps.

Initialization was the first step, and required the most coordination between modules on the HPC. A Python script was used to open STK, identify the program input parameters, and select the algorithms to execute. A combination of STK generated reports was used throughout this process. The reports were necessary to identify which sensors could detect and identify an RSO at each time step. Moon phase, lunar zenith angle, lunar phase angle, target zenith angle, solar phase angle, range to target, angle between target and observer, azimuth data, and elevation data were all used to calculate realistic access from every sensor to all 813 RSOs identified in the target deck. By utilizing an HPC to run the initialization step of this methodology, computational resources were accelerated by a factor of 170. In order to maximize the utility of the HPC, an internal batch scheduling system prioritized jobs based on the number of cores needed (Stern et al., 2017). This ensured the requested HPC nodes were utilized as close to 100% as possible.

Operation on the HPC required a Linux based Python script to open the STK program, input the desired parameters through AGI's "connect" interface, and activate the subsequent generation and evaluation modules. The input parameters included estimated run time, RSO orbital parameters, evaluation window dates, time step, and architecture boundaries. These parameters were fed into the HPC scheduler and the STK program to define access from every possible sensor to every RSO at each time step throughout the simulation; 24 hours sampled every 30 seconds.

Next, the access data from every possible sensor to every target was calculated. This generated a massive amount of data that was then filtered, sorted, and analyzed. Tens of thousands of reports contained the data required to perform access calculations for every sensor to every RSO at every time step. After the data was analyzed, three objective functions were evaluated. For this research, the three objectives were to minimize total architecture cost, mean detectable object size, and minimize overall latency of the system. The genetic algorithm identified which architecture had the highest score when evaluated equally against these three objectives.

Since any robust architecture will identify several assets that can observe a given target at a particular time, a scheduler was needed to identify and prioritize which sensor should observe which target. Additionally, there may be time steps where an RSO cannot be seen by any sensor. In order to optimize the architecture, a simple latency-based scheduler was implemented for this research. The "greedy" scheduler identifies which RSO has gone the longest amount of time without an observation and schedules the first available sensor to observe that RSO. This process repeats until every available sensor is scheduled. Then, simulated time steps forward one increment of 30 seconds and the entire scheduling process repeats. The results of the scheduling algorithm provide both the overall mean latency of the observations and the mean target size observable by the architecture.

The smallest size object that can be detected varies for each asset contained in any GEO SSA architecture. Sensor size, distance to target, sun incidence angle, and angle between target and observer are the primary drivers for RSO detection capability. This analysis used an optical sensor Signal-to-Noise Ratio (SNR) of 6 as a minimal threshold for RSO detection. Any RSO with a SNR of 6 or greater was assumed to be observable by that sensor.

The capability of any ground-based sensor to detect RSOs in GEO also varies depending on atmospheric transmission. The Laser Environmental Effects Definition and Reference (LEEDR) toolset was used to estimate the atmospheric transmission for each possible ground telescope location. Additionally, previous research restricted ground site operation during daylight hours. This research expanded the operational capability of ground sensors by allowing imaging of RSOs during twilight. Space-based sensors have the capability to operate 24/7 and were only restricted from observing targets within a 40° exclusion angle of the Sun.

The second step for this methodology identified candidate architectures to evaluate. The baseline methodology used a population size of 96 for 100 generations. Every trial evaluated 9,600 architectures on total architecture cost, mean detectable object size, and overall latency of the system. Pisacane (2016) details how a score can be assigned for each architecture that varies depending on sensor performance for RSOs in GEO. Every candidate architecture can be evaluated based on how that architecture performs against the three objectives: cost, detection size, and latency. Each of the three objectives was evaluated independently then normalized using a Single Attribute Value Function (SAVF) to obtain a value score (0.0 – 1.0) for each objective. These scores were then combined with equal weights to determine the total architecture value. Since there are 10^{22} total possible sensor combinations, a “brute force” complete search was not possible. To combat this, a Python implementation of a MOGA optimizer called *Inspyred* (Garrett, 2012) was used to intelligently search the design space. Early trials determined reasonable values for population size, genetic mutation rate, crossover parameters, scheduling algorithm, selection criteria, and scoring criteria. This provides the GA with all the necessary parameters to generate architectures, score the architectures, crossover the highest scored architectures genes, randomly mutate those architectures, and repeat for each generation.

A 95% learning curve was applied to satellite acquisition costs. This realistic assessment of satellite acquisition costs reduces the per satellite cost as more satellites are built. The learning curve formula is defined in Eq 1:

$$Total\ lot\ cost = T1\ \times N^{1+\frac{\ln 0.95}{\ln 2}} \qquad \text{Eq 1.}$$

where

$T1 =$ the production cost of the first satellite

$N =$ number of satellites

Refinement of this methodology allowed additional analysis of GEO SSA characteristics as well as expansion into additional trade spaces. For this research, five enhancements increase the utility of the refined methodology. The first enhancement added limited daylight imaging to the ground site detection capability. Daylight imaging allows detection of RSOs longer into the dawn and earlier prior to dusk. Specifically, the periods of Astronomical Dawn, Nautical Dawn, Civil Dawn, Civil Dusk, Nautical Dusk, and Astronomical Dusk were added to the previous Umbra-only ground site operation. Depending on ground site latitude location, this added approximately 71.8 minutes of ground telescope operation on either side of night.

The next three enhancements were applied to the space component of the architecture. First, the previous research limited any particular architecture to a maximum of four satellites in a plane. This was expanded to six to further explore the trade space since previous results frequently maximized this orbital characteristic. Secondly, the SSO regime was eliminated as a design parameter since it was rarely selected over the other orbit options (Stern et al., 2017).

The final space-based enhancement added two planes with a capacity of six satellites per plane in a GPO configuration. This orbit provided an average percent access to the GEO belt of 89%. This is significantly higher than the percent access provided from SSO, 57%, and near GEO, 75% (Vallado et al., 2016).

These space element changes, combined with the increased ground site operation improved the total system collection capability. It also increased the trade space from 10^{19} total possible sensor combinations to 10^{22}. The increased time needed to search this larger trade space was offset by efficiencies gained from the refined methodology. These efficiencies were the final enhancement to the methodology and included improvements and refinement of the optimizer, doubling the population size to 192, halving the number of generations to 50, accelerated data verification, increased parallelization via distribution to more processing nodes, and improved data generation reliability. Early trials indicated that reduction in the number of generations to 50 had little impact on the final selected architecture. Data generation was accelerated by a factor of six while data evaluation was accelerated by a factor of three over the previous study. The total number of architectures evaluated per trial was still 9,696 and the best value architectures were typically discovered consistently by generation ~25, as can be seen in Figure 4.

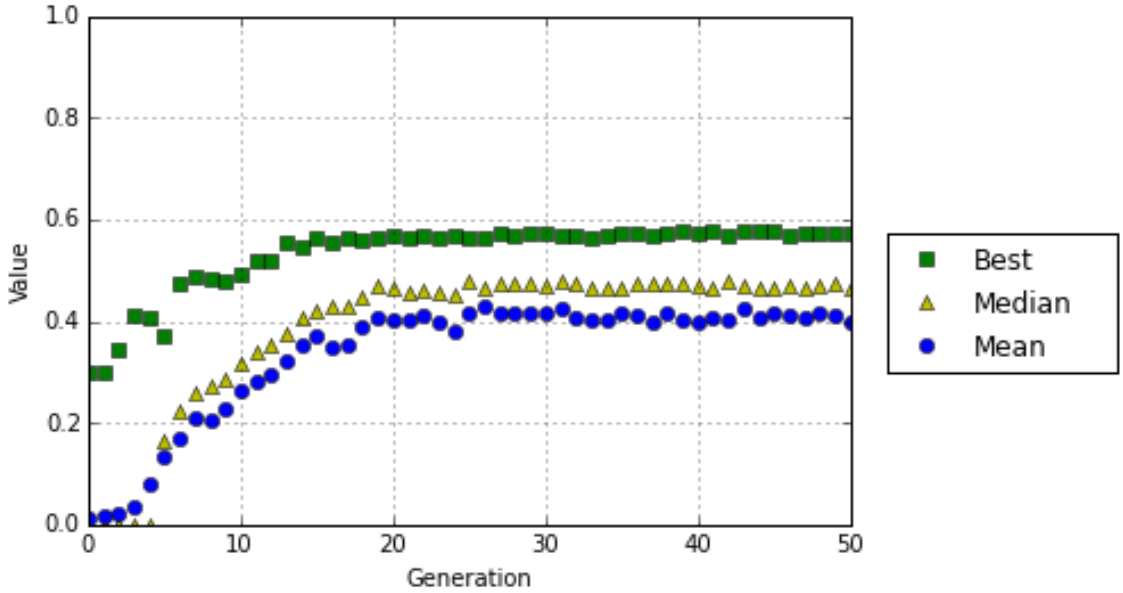

Figure 4. Value Trends by generation, 813 RSO targets, 0.05 mutation rate, population of 192, and 50 generations

These enhancements greatly increased the capability of this methodology. An optimization run that simulates 9600 architectures for 24 hours previously required three days to complete but can now be accomplished in a single day. This enabled an expansion of the trade space to 1000 times larger than previous research which in turn resulted in better performing GEO SSA architectures at a similar or reduced cost.

IV. Analysis and Results

The results detailed in this paper first extend the baseline results (Stern et al., 2017) and then evaluates three sets of new experiments. Due to limitations of the MOGA used in the Stern et al. (2017) research, the longest scenario runtime possible was a single 24 hour period. In order to minimize the limitations of this approach, their research ran an STK scenario one day on the spring equinox (21 March) and one day on the summer solstice (21 June). This approach bounds the limitations and advantages of any particular orbital regime due to Earth-Sun angel variations. One example of this is the poor performance of an Equatorial LEO satellite on the equinox. The results of this equinox and solstice simulation (shown in Table 1) highlight how the optimal architecture varies depending on the Earth-Sun orientation. Once the solstice and equinox trials were simulated and verified, a single additional run was completed on 11 May to determine performance for a day between the solstice and equinox.

Table 1. Multi-Objective Results, Expanding (Stern et al., 2017) with an additional trial on 11 May.

	Equinox 21 March	11 May	Solstice 21 June
Number of near GEO Satellites	4	3	3
Aperture Diameter (m)	0.6	0.45	0.45
Delta Altitude from GEO (km)	+1000	+500	+1000
Number of LEO Equatorial Satellites		4	3
Aperture Diameter (m)		0.3	0.3
Altitude (km)		700	900
Number of Sun Synch Orbit Satellites			
Telescopes at Socorro, NM	4	3	4
Aperture Diameter (m)	1.0	0.5	1.0
Telescopes at Siding Spring			4
Aperture Diameter (m)			1.0
Telescopes at Paranal Chile	4		4
Aperture Diameter (m)	1.0		1.0
Telescopes at Mt. Graham	3	4	4
Aperture Diameter (m)	1.0	1.0	1.0
Telescopes at Indian Astro. Obs (IAO)	4	3	4
Aperture Diameter (m)	1.0	0.5	0.5
Telescopes at Mauna Kea	4	3	4
Aperture Diameter (m)	1.0	0.5	1.0
Telescopes at La Palma		3	3
Aperture Diameter (m)		1.5	1.0
Telescopes at Haleakala	4	4	3
Aperture Diameter (m)	1.0	1.0	1.0
Telescopes at Diego Garcia	4	3	1
Aperture Diameter (m)	1.0	1.0	0.5
Architecture Performance			
RSO Size (cm)	52.3	53.6	60.5
Latency (min)	81.0	47.0	42.8
Cost ($B)	1.49	1.75	1.56
Value	0.302	0.393	0.399

For this research, the most cost-effective telescope size for a ground-based SSA sensor has an aperture of 1m. The exclusion of any SSO satellites for this initial trial run is understandable given the previously identified advantages of an equatorial LEO satellite and a near GEO satellite. Maximizing the number of near GEO assets for the equinox case is expected given the limitations of an equatorial LEO satellite. It is interesting to note that the optimal architecture for 11 May keeps a similar near GEO architecture from the solstice, but also favors maximizing the equatorial LEO satellites. It also continues the trend of not selecting any satellites in SSO. For ground, the reduction of 1.0-meter telescopes is compensated by adding nine 0.5-meter telescopes and three 1.5-meter telescopes.

The refined methodology used for the remaining results was intended to explore an additional trade space, enhance total system collection capability, and remove the limitation of four satellites per plane. In order to prevent time of year bias from driving the solution, 18 24-hour trials were performed on varying days of the year. Three days per month from January to June encompass the complete Earth-Sun angle variations since July to December will mirror the first six months of the year. Ground site operation was expanded to include twilight. Two planes of GPO satellites with a maximum of six satellites per plane was added to the trade space. The maximum satellites per plane in equatorial LEO and near GEO was set to six to match the GPO satellite per plane maximum. The parameters including the space-based telescope 40° solar exclusion angle, the 95% satellite production learning curve, and the ground telescope 20° minimum elevation angle were all maintained from the baseline methodology. See Table 2.

Table 2. Multi-Objective Results with aggregated counts of sensors (Jan-Jun).

Date	Ground Telescopes			Space Telescopes		Architecture Performance			
	0.5m	1.0m	1.5+m	# of GPO	# of LEO/GEO	Size (cm)	Latency (min)	Cost ($B)	Value (0-1)
1 Jan	5	6	8	12		29.4	40.7	1.11	0.59
11 Jan	4	20		12		28.1	39.2	1.04	0.61
21 Jan		3	10	12		27.4	51.1	1.15	0.56
1 Feb		13	5	12		26.9	48.6	1.56	0.58
11 Feb		19	2	12		24.3	51.5	1.14	0.58
21 Feb		7	7	12		31.0	60.3	1.10	0.52
1 Mar			5	12		20.1	78.8	0.97	0.51
11 Mar		5	9	10		19.2	82.5	1.04	0.49
21 Mar		3	7	12		26.0	83.8	1.04	0.46
1 Apr		11	4	12		23.1	70.7	1.04	0.52
11 Apr		19	2	12		21.9	54.7	1.07	0.58
21 Apr		9	4	12		33.5	52.8	1.10	0.53
1 May		18	1	12		25.1	49.0	1.04	0.59
11 May		13	6	12		23.7	46.4	1.11	0.60
21 May	3	13	5	12		37.4	44.2	1.10	0.55
1J un		10	10	12		21.7	42.3	1.19	0.61
11 Jun		15	3	12		25.0	43.2	1.07	0.61
21 Jun	2	6	6	12		33.8	43.9	1.17	0.56

The first thing that stands out is the maximization of the GPO regime for all trials except 11 March. This is most likely due to the restriction of a 40° solar exclusion angle on all satellites. This restriction impacts the GPO satellites less due to the geometry of the observing satellites in that plane to the RSOs in GEO.

The advantages of the GPO SSA constellation are emphasized when comparing results directly with the previous obtained optimal architectures using the baseline methodology, based on ground telescopes, Equatorial LEO and near GEO sensors. Table 3 directly compares these results. GPO shows much better performance in mean detection size with similar latency, less cost and higher value.

Table 3. Baseline (Ground, Equatorial LEO and near GEO) compared to refined methodology often selecting maximum numbers of GPO.

Date	Method	Ground Telescopes	Space Telescopes		Architecture Performance			
		# Total	# of GPO	# of LEO/GEO	Size (cm)	Latency (min)	Cost ($B)	Value (0-1)
21 Mar	Baseline LEO/GEO	29		4	52.3	81.0	1.49	0.30
	Refined GPO	10	12		26.0	83.8	1.04	0.46
11 May	Baseline LEO/GEO	23		7	53.6	47.0	1.75	0.39
	Refined GPO	19	12		23.7	46.4	1.11	0.60
21 Jun	Baseline LEO/GEO	31		6	60.5	42.8	1.56	0.40
	Refined GPO	14	12		33.8	43.9	1.17	0.56

The refined methodology increases the overall value of the GEO SSA architecture for all three dates previously analyzed. This value increase is driven by a decreased total architecture cost and an increased architecture RSO size detection capability. The total number of ground telescopes was reduced and the total number of space telescopes in GPO was maximized in all cases. This demonstrates the increased capability of a GPO satellite compared with LEO or near GEO satellites. Since the GPO satellites are not affected by the 40° solar exclusion angle as dramatically as equatorial LEO and near GEO, they can offer a better RSO detection capability.

The GPO regime has the greatest potential reduction in per unit cost when applying the satellite learning curve since the maximum number of GPO satellites (12) was often identified as optimal. This was likely a contributing factor to the selection of that orbit. In order to determine the significance of this contributing factor, an experiment was conducted to examine the impact of the production cost learning curve. The results in Table 4 use an identical methodology as the results in Table 2 except the learning curve was changed from 0.95 to 1.00. This eliminated any potential bias towards space-based sensors because of the learning curve.

Table 4. Multi-Objective Results with Elimination of Satellite Learning Curve

Date	Ground Telescopes			Space Telescopes		Architecture Performance			
	0.5m	1.0m	1.5+m	# of GPO	# of LEO/GEO	Size (cm)	Latency (min)	Cost ($B)	Value (0-1)
1 Jan	9	16		12		36.1	36.5	1.19	0.57
11 Jan		15	6	12		23.9	42.9	1.35	0.58
21 Jan		12	6	12		30.6	45.4	1.32	0.55
1 Feb	2	13	6	12		26.5	48.6	1.33	0.55
11 Feb	1	18	1	10		25.7	55.4	1.12	0.56
21 Feb		10	2	12		32.7	61.6	1.08	0.49
1 Mar		18		10		29.2	69.2	1.08	0.49
11 Mar		12	3	8		21.8	84.8	0.99	0.48
21 Mar	7	12	4		5 (0.30)	26.0	83.8	1.34	0.46
1 Apr		15	2	10		25.4	70.2	1.16	0.50
11 Apr	2	10	4	12		24.0	54.7	1.24	0.55
21 Apr		5	5	12		29.5	59.8	1.24	0.51
1 May		10	5	12		22.4	52.7	1.26	0.56
11 May	4	13	3	12		26.7	46.8	1.24	0.57
21 May		13	3	12		35.3	46.3	1.27	0.53
1 Jun		19		12		25.1	43.6	1.21	0.59
11 Jun		13	5	12		24.0	42.6	1.30	0.59
21 Jun	1	7	6	12		32.9	44.8	1.38	0.53

The results show that even without the learning curve, the GPO satellites are preferred in all cases except on the equinox. The selection of three equatorial LEO satellites on the equinox does match earlier results from Stern et al. (2017) but does not match their final data set. This difference illustrates the variability involved when analyzing such a large trade space. In all cases, the value of the architecture was increased when including a 95% learning curve. The closest value between the two runs occurs on the equinox where elimination of the learning curve decreased the architecture value from 0.4582 to 0.4552. The fact that these two vastly different architectures have such a close score in value partially explains why the optimizer selects equatorial LEO and near GEO regimes over GPO on the equinox. Another interesting observation is that all the runs with the learning curve set at 95% were cheaper except for 11 February, 1 March, and 11 March. These dates correspond to the only dates (other than the equinox) where the total number of GPO satellites was decreased. All this leads to the conclusion that the optimizer selected the GPO regime over equatorial LEO and near GEO primarily because of the increased utility of that orbital plane geometry and not primarily because of the 95% satellite learning curve.

In order to define one GEO SSA architecture that is optimal year-round, the most common architectural components were selected. The architecture defined on 1 February using a satellite learning curve and 11 June without a satellite learning curve was the most commonly selected architecture by the optimizer. Because it was the most commonly selected architecture, it is likely the highest performing architecture throughout the year. Future work can simulate this architecture on every day of the year and compare that average performance to any other architecture's average performance to guarantee any selected architecture is optimal. For this research, the most commonly selected architecture is considered to have the most optimal year-

round performance. Two planes with six satellites per plane in GPO was identified as the space component to this optimal architecture. These two planes are separated by a 90° offset longitude of ascending node and mean anomaly. The complete orbital elements are: eccentricity equal to 0.000988, semi-major axis of 42,457 kilometers, 89° inclination, a longitude of ascending node set to 0° and 90° respectively, an argument of periapsis of 180°, and a mean anomaly set to 0° and 90° respectively. The ground component includes thirteen 1.0-meter aperture telescope and five 1.5-meter aperture telescope distributed at various locations around the globe. While other combinations of ground sensors are optimal on different days, this specific architecture was the only combination of ground sensors selected by the optimizer on two independent days.

Modeling and simulation of complex GEO SSA architectures provides a unique ability to understand the costs and benefits of different combinations of sensor technologies. Visualizing the performance and cost tradeoffs from different components of the architecture is difficult since the trade space is so large and contains so many architectural elements. A parallel coordinates diagram can help visualize paths through multiple inputs in order to achieve a selected output. The relationship between different numbers of ground aperture sensors and different orbital regimes for value scores between 0.40 and 0.61 is highlighted in green in Figure 5. Darker lines indicate a stronger correlation to architectures with the high value score highlighted in green.

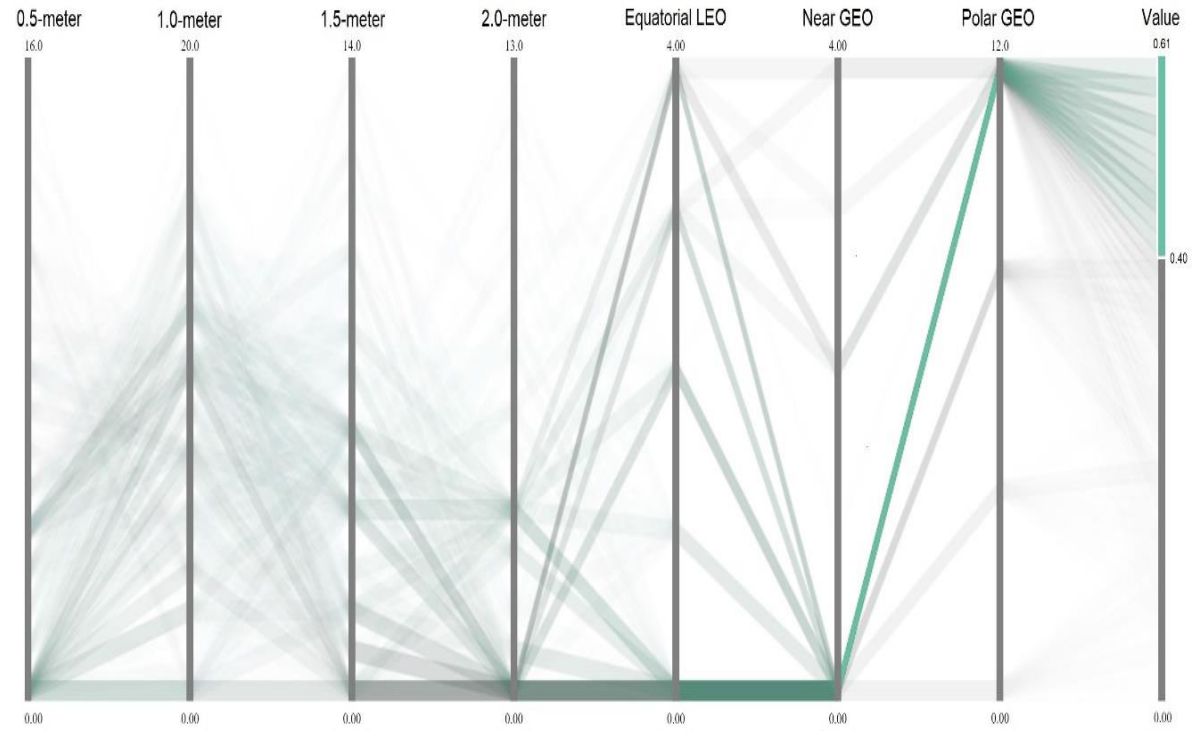

Figure 5. Parallel Coordinates Diagram for Architecture Elements

All architectures that scored higher than 0.40 in equal weighted value used a 12-satellite GPO space component. This exemplifies the utility of this specific orbital regime. The importance of the 1.0-meter aperture ground telescope is clearly seen from the spike in total number of 1.0-meter aperture ground telescopes. The dark green line emanating from the base of the near GEO column illustrates that very few high-scoring architectures used a near GEO satellite constellation.

The selection of specific ground telescope locations and aperture sizes is dependent on their complement with a twelve-satellite GPO constellation divided equally into two planes. Other ground telescope locations and aperture sizes can be selected and combined with the GPO constellation but should be considered a complementary package with the space component only as a complete set. The identified optimal architectures are only optimal architectures for the single day that the architecture was evaluated on. Each of these optimal architectures have varying performance throughout the year. Figure 6 illustrates the performance, cost, and value variability for each optimal architecture.

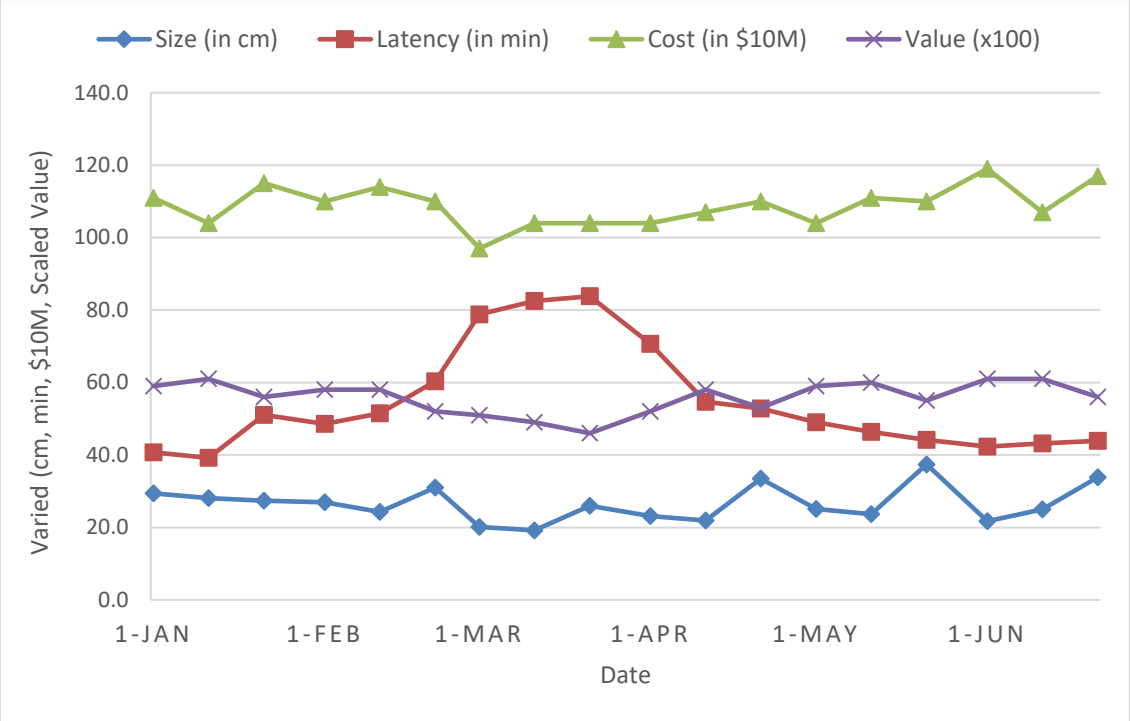

Figure 6. Optimal Architecture Performance Variation by Time

In Figure 6, lower size and latency correspond to better performing architectures. The total system cost is identified in tens of millions of dollars. The value score is normalized from 0 to 100 to show the overall value of the architecture when weighing all three performance criteria equally. The GEO RSOs behind the shadow of the Earth clearly drives up the latency performance on days near the equinox. This negatively affects the value of the optimal architecture for that day. However, these architectures are still considered the optimal architecture for that particular day even though they have a lower value score when compared to optimal architectures near the solstice. Since the optimal combination of ground-based and space-based sensors change throughout the year, this research identified the most commonly selected architecture as the most-likely year-round optimal architecture.

V. Conclusion

The intent of this research was to improve knowledge of cost and performance tradeoffs for GEO SSA architectures by answering two research questions:

1. What combination of ground and space-based sensors provide the most cost-effective architecture for a high-fidelity GEO SSA system?
2. How does the optimal architecture change throughout the year because of Earth-Sun angle variations?

Various combinations of ground and space-based sensors were found on different days of the year. One architecture was selected as optimal for two independent days of the year and therefore selected as the most cost-effective architecture for a high-fidelity GEO SSA system. This architecture includes twelve 0.15-meter aperture sensors hosted on polar GEO satellites in two equal planes combined with thirteen 1.0-meter and five 1.5-meter aperture ground telescopes at varying locations around the globe.

The refined methodology used in this research searched a 10^{22} trade space. This expanded search identified architectures that had an increased value by nearly 50%. Value was calculated using an equal weighting on all three performance criteria: total system cost, mean detectable object size, and the time lag between subsequent RSO observations. The identified GPO satellites were a large contributor to the overall increase in value. When performance is held constant, a GPO satellite constellation offers a 22.4% reduction in total system cost when compared to SSO, equatorial LEO, and near GEO.

The results of this research demonstrate the utility of model-based GEO SSA architecture evaluation. Running these analyses on HPCs compounds that utility. Trade space analysis and architecture evaluation on this scale would not be possible without the use of the HPC. The ability to run thousands of simulations in parallel allows analysis of architecture perturbations in a timely fashion. The addition of visualization tools such as parallel coordinates diagrams greatly improves the human interpretability of the large data set results. This leads to faster problem orientation and solution identification. A single four-core desktop machine would take more than 100 years to repeat the modeling, simulation, and evaluation conducted in this research.

These results form a complete ground and space-based system architecture with the greatest value in pursuit of a high-fidelity GEO SSA system. This architecture mirrors other optimal architectures found on different days of the year. The performance of this specific architecture is not guaranteed to be the most optimal architecture on any specific day but should offer the most optimal year-round performance.

The methodology refined through this research has a much greater utility than just as a tool for GEO SSA architecture evaluation. A portion of this methodology contains a tool set for efficient evaluation of very large trade spaces. Application of this tool set could be applied to any large data set; it is not limited exclusively to GEO SSA architecture analysis. It can be used as a source selection tool to evaluate opposing contractor bids, a simulation tool for efficient evaluation of very large trade spaces, or an analysis workbench for comparison of emerging technologies. Scripting and parallel high-performance computing opens the possibility of solving an entirely new class of problems.

Disclaimer
The views expressed in this paper are those of the authors and do not reflect the official policy or position of the US Air Force, Department of Defense or the US Government.

Acknowledgement
We sincerely thank Analytical Graphics Inc. for allowing us to use Systems Tool Kit Engine that allowed parallel simulation on a high performance computer.

Funding
The authors received no financial support for the research, authorship, and/or publication of this article.

Declaration of Conflicting Interests
The authors declare that there is no conflict of interest.

References
Abbot, R. I., & Wallace, T. P. (2007). Decision support in space situational awareness. *Lincoln Laboratory Journal*, *16* (2), 297–336.

Ackermann, M. R., Kiziah, R. R., Zimmer, P. C., McGraw, J. T., & Cox, D. D. (2015). A systematic examination of ground-based and space-based approaches to optical detection. *31st Space Symposium*, 1–46.

Baird, M. A. (2013). Maintaining space situational awareness and taking it to the next level. *Air and Space Power Journal*, *27*(5), 50–72. Retrieved from http://www.dtic.mil/docs/citations/ADA625687

Barry, E. (2017, February 15). India launches 104 satellites from a single rocket, ramping up a space race. *The New York Times.* Retrieved from https://www.nytimes.com/2017/02/15/world/asia/india-satellites-rocket.html?_r=0

Brissett, W. (2017, August). A closer watch on space. *Air Force Magazine.* Retrieved from http://www.airforcemag.com/MagazineArchive/Pages/2017/August 2017/A-Closer-Watch-on-Space.aspx

Clark, S. (2017, August 30). Minotaur 4 blasts off from Cape Canaveral. *Spaceflight Now*. Retrieved from https://spaceflightnow.com/2017/08/30/photos-minotaur-4-blasts-off-from-cape-canaveral/

Dacres, K. D. (2016). From here to ubiquity: The American Space Renaissance Act & its impact on the future of space. Forum on Air & Space Law, Annual Conference 2016, *4945*, 2015–2016.

Früh, C., & Jah, M. K. (2014). Detection probability of Earth-orbiting objects using optical sensors. *Advances in the Astronautical Sciences* (150, pp. 3–14). Retrieved from http://www.univelt.com/book=4267

Garcia, J. J., & Tolk, A. (2015). Executable architectures in executable context enabling fit-for-purpose and portfolio assessment. *Journal of Defense Modeling and Simulation*, *12*(2), 91–107. https://doi.org/10.1177/1548512913491340

Garrett, A. (2012). Inspyred. Retrieved from https://pypi.python.org/pypi/inspyred

John, E. (2002). A sea of peace or a theater of war?: Dealing with the Inevitable Conflict in Space. Retrieved from https://www.thefreelibrary.com/A+sea+of+peace+or+a+theater+of+war%3f+Dealing+with+the+inevitable...-a094269862

Joint Functional Component Command for Space. (2016). *Geosynchronous Report*. Retrieved from https://www.space-track.org/

Marlow, W. A., Carlton, A. K., Yoon, H., Clark, J. R., Haughwout, C. A., Cahoy, K. L., … Morzinski, K. M. (2017). Laser-guides-star satellite for ground-based adaptive optics imaging of geosynchronous satellites. *Journal of Spacecraft and Rockets*, *54*(3), 621–639. https://doi.org/10.2514/1.A33680

Pisacane, V. L. (2016). *The Space Environment and Its Effects on Space Systems* (2nd Ed). Reston, VA: American Institute of Aeronautics and Astronautics, Inc.

Scott, R., Wallace, B., Sale, M., & Levesque, M. (2013). Toward microsatellite based space situational awareness. *Advanced Maui Optical and Space Surveillance Technologies Conference*. Retrieved from https://amostech.com/2013-technical-papers/

Smith, M. (2017). Top Air Force officials: Space is a warfighting domain. Retrieved from https://spacepolicyonline.com/news/top-air-force-officials-space-now-is-a-warfighting-domain/

Stahl, H., Henrichs, T., & Luedtke, A. (2011). Update on parametric cost models for space telescopes. *SPIE Optical*. Retrieved from http://reviews.spiedigitallibrary.org/pdfaccess.ashx?url=/data/conferences/spiep/62821/81460f_1.pdf

Stern, J., Wachtel, S., Colombi, J., Meyer, D., & Cobb, R. (2017). Multi-objective optimization of geosynchronous Earth orbit space situational awareness system architectures. Redondo Beach, CA: 15th Annual Conference on Systems Engineering (CSER) Research. Retrieved from 10.1007/978-3-319-62217-0_42

Tanaka, K. (2017, June). Applicability of remote sensing policies to space situational awareness. *Space Policy*, 1–9. https://doi.org/10.1016/j.spacepol.2017.06.002

Thompson, R. E., Colombi, J. M., Black, J., & Ayres, B. J. (2015). Disaggregated space system concept optimization: Model-based conceptual design methods. *Systems Engineering*, *18*(6), 549–567. https://doi.org/10.1002/sys.21310

Vallado, D. A., Ackermann, M. R., Cefola, P. J., & Kiziah, R. R. (2016). Orbital strategies to mitigate the solar exclusion effect on space-based observation of the geosynchronous belt.

van Belle, G. T., Meinel, A. B., & Meinel, M. P. (2004). The scaling relationship between telescope cost and aperture size for very large telescopes. *Astronomical Telescopes and Instrumentation*, *5489*, 563–570. https://doi.org/10.1117/12.552181

Wiedemann, C. (2018). Space Debris. Braunschweig, Germany: Institute of Space Systems, Braunschweig University of Technology.